

Rapid prediction of inelastic bending moments in RC beams considering cracking

K. A. Patel^{1a}, Sandeep Chaudhary^{*2} and A. K. Nagpal^{1b}

¹Civil Engineering Department, Indian Institute of Technology Delhi, New Delhi 110016, India

²Civil Engineering Department, Malaviya National Institute of Technology Jaipur, Jaipur 302017, India

(Received February 24, 2016, Revised September 14, 2016, Accepted September 27, 2016)

Abstract. A methodology using neural networks has been proposed for rapid prediction of inelastic bending moments in reinforced concrete continuous beams subjected to service load. The closed form expressions obtained from the trained neural networks take into account cracking in concrete at in-span and at near the internal supports and tension stiffening effect. The expressions predict the inelastic moments (considering the concrete cracking) from the elastic moments (neglecting the concrete cracking) at supports. Three separate neural networks are trained since these have been postulated to represent all the beams having any number of spans. The training, validating, and testing data sets for the neural networks are generated using an analytical-numerical procedure of analysis. The proposed expressions are verified for example beams of different number of spans and cross-section properties and the errors are found to be small. The proposed expressions, at minimal input data and computation effort, yield results that are close to FEM results. The expressions can be used in preliminary every day design as they enable a rapid prediction of inelastic moments and require a computational effort that is a fraction of that required for the available methods in literature.

Keywords: bending moment; closed form expression; cracking; neural network; reinforced concrete; service load

1. Introduction

Reinforced Concrete (RC) beams are widely used in the construction of buildings and bridges. In a continuous beam, the hogging moment occurs near the ends of the members whereas the sagging moment occurs in the middle portion of the members. At service load, concrete in tensile zone generally gets cracked owing to moments in the zone being higher than the cracking moments. For example, in an intermediate span of a RC continuous beam, cracking may occur near the internal supports and in the middle portion of a span as shown in Fig. 1. Due to this cracking, there can be a significant amount of moment redistribution in the continuous beams.

A large number of procedures are available in the literature for the analysis of RC beams, which

*Corresponding author, Ph. D., E-mail: schaudhary.ce@mnit.ac.in

^aPh. D., E-mail: iitd.kashyap@gmail.com

^bPh. D., E-mail: aknagpal@civil.iitd.ac.in

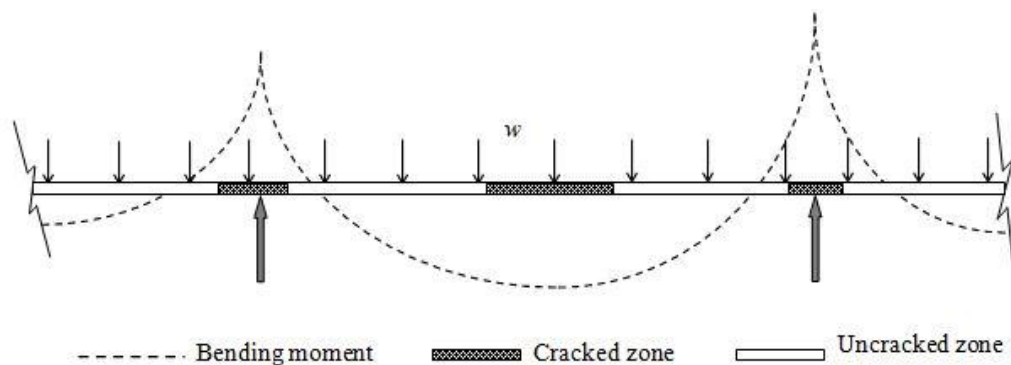


Fig. 1 A typical intermediate span of a RC beam with loads, bending moment, and possible cracked-uncracked zones

take into account the concrete cracking and other non-linear effects such as aggregate interlock, dowel action, bond-slip, etc. In Type 1 procedures (Wang and Hsu 2001, Yang and Chen 2005, Stramandinoli and Rovere 2008, 2012, Mohr *et al.* 2010, Casanova *et al.* 2012, Dai *et al.* 2012), members are discretized into a number of elements along the length or across the cross-section or both along the length and across the cross-section. In Type 2 procedures (Chan *et al.* 2000a, b, Tanrikulu *et al.* 2000, Dundar and Kara 2007, Kara and Dundar 2009, 2010), the effective moment of inertia of members (representing average moment of inertia along the member length) and the transformed section properties are considered. Both these types of procedures are based either on an incremental or iterative approach and therefore, require a computational effort, which is many times more than that required for the elastic analysis (neglecting cracking).

In order to deal with serviceability limit state of cracking, ACI 318 (2005) gives an empirical relation for limiting value of reinforcement spacing, s , in which stress in steel, f_s , on tension face is one of the parameters. It is implicit that undistributed moments would be used in evaluation of f_s . It would be rational to develop relation which would make use of distributed moments in evaluation of S . No procedure exists for rapid evaluation of inelastic moments resulting from cracking. The use of closed form expressions obtained from the trained neural networks may be made in such cases to rapidly estimate the inelastic moments of design interest for use in everyday design. It is expected that the present methodology which yields rapid estimation of inelastic moments would give impetus to develop more rational relation that make use of inelastic moments rather than elastic moments.

Neural networks have been extensively used in the field of structural engineering to predict the parameters without any rigorous analysis and experiments (Chaudhary *et al.* 2007, 2014, Pendharkar *et al.* 2007, 2010, 2011, 2015, Kim *et al.* 2009, Saechai *et al.* 2011, 2012, Khan 2012, Mohammadhassani *et al.* 2013a, b, Joshi *et al.* 2014, Tohidi and Sharifi 2015). Many researchers have proposed closed form expressions using the weight matrices and activated function of the trained neural network. Some of the closed form expressions obtained from the trained neural networks have been used by researchers for determination of distortional buckling stress in cold-formed steel members (Pala 2006), estimation of ultimate pure bending of fabricated and cold-formed steel circular tubes (Shahin and Elchalakani 2008), prediction of base shear of steel frame structures (Caglar *et al.* 2009), estimation of distortional buckling stress in elliptical hollow section tubes (Dias and Silvestre 2011), evaluation of deflections in composite bridges considering

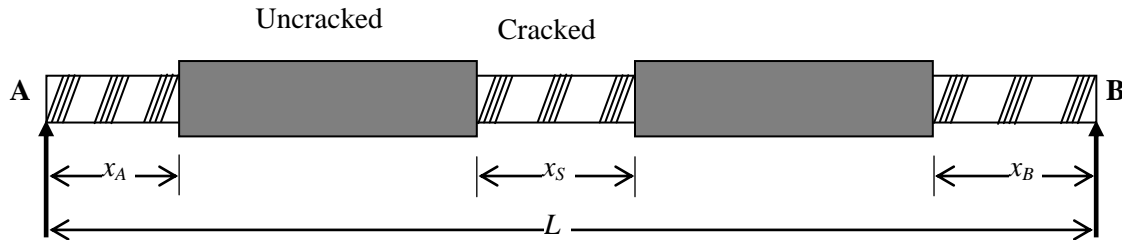


Fig. 2 A cracked span length beam element

nonlinear effects like flexibility of shear connectors, concrete cracking and shear lag effect (Tadesse *et al.* 2012, Gupta *et al.* 2013, 2015), and prediction of effective moment of inertia in RC beams (Patel *et al.* 2015). Such closed form expressions are useful to estimate the quantities of design interest for use in everyday design with acceptable accuracy. These studies reveal the strength of neural networks in predicting the solutions of different structural engineering problems.

In this paper, a methodology using neural networks has been proposed for rapid prediction of inelastic bending moments in RC continuous beams subjected to service load. The closed form expressions obtained from the trained neural networks take into account cracking in concrete and tension stiffening effect. The expressions predict the inelastic moments, M^{in} (considering the concrete cracking) from the elastic moments, M^{el} (neglecting the concrete cracking) at supports. M^{el} , in turn, can be obtained from any of the readily available software. The expressions enable rapid estimation of inelastic moments and require a computational effort that is a fraction of that required for Type 1 and Type 2 procedures available in the literature. The proposed expressions have been verified for a number of example beams. The errors are shown to be small for practical purposes. The methodology can be extended for large RC building frames where a very significant saving in computational effort would result.

2. Analytical-numerical procedure for analysis of RC beams

For generalized and efficient neural networks, a huge number of training, validating, and testing data sets are required for which a highly computationally efficient method is desirable. Recently, Patel *et al.* (2014) developed an analytical-numerical procedure to take into account concrete cracking within the spans and near the internal supports and reinforcement variation along the span in RC beams. The procedure is analytical at the element level and numerical at the structural level. A cracked span length beam element, consisting of five zones (three cracked zones of lengths x_A , x_B at the ends A and B respectively and x_S at an in-span position, and two uncracked zones in between the cracked zones), (Fig. 2) has been used in the procedure. The closed form expressions for crack lengths, flexibility matrix coefficients, end displacements, and mid-span deflection of the cracked span length beam element are derived and used in the procedure. Tension stiffening effect is also taken into account by evaluating average interpolation coefficients for the cracked zones. The analysis is carried out using an iterative method.

Consider, a typical iterative cycle. A displacement analysis is carried out in the beginning of the cycle for the out-of-balance force vector of the RC beam at the end of the previous cycle.

Revised force vector and displacement vector are obtained by adding the force vector and displacement vector obtained from this analysis to the force vector and displacement vector at the end of previous cycle. Crack lengths and interpolation coefficients are then updated according to the revised force vector (Varshney *et al.* 2013).

Changes in the cracking state of the sections (cracked or uncracked) and thereby in the end rotations of the beam elements lead to the difference between the displacement vector of these elements obtained from the displacement analysis and that obtained by the principle of virtual work involving integration of curvature diagram of a member. The out-of-balance force vector corresponding to this error in displacement vector can be obtained using the revised flexibility matrix of the beam element.

The out-of-balance force vector of the continuous RC beam (obtained by assembling the out-of-balance force vector of the beam elements) should be within permissible limit (Bathe 2002) for the iterative process to terminate; otherwise a new cycle is started. Required results are obtained after convergence is achieved.

The procedure has been validated by comparison with the experimental and numerical results available in literature along with finite element method (FEM) results. The computational time required by the procedure is shown to be a small fraction of that required in the FEM.

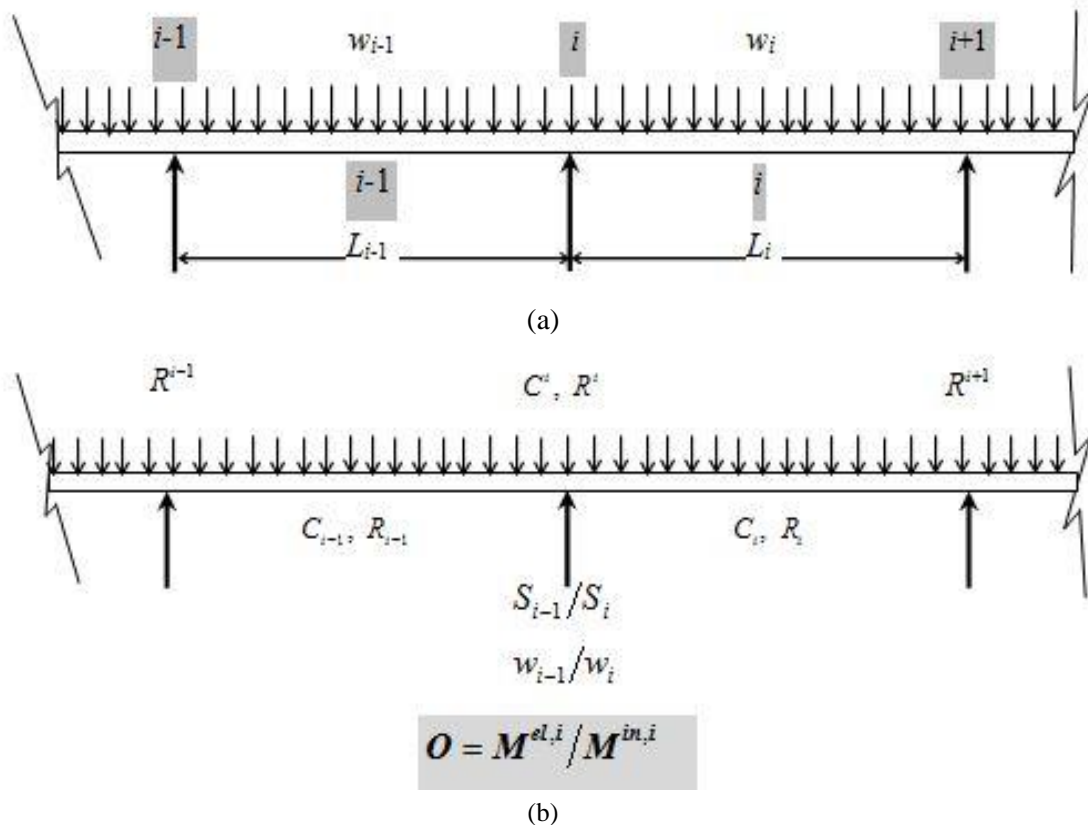


Fig. 3(a) A typical span of a continuous beam and (b) schematic representation of input and output parameters

Table 1 Practical range and sampling point of probable structural input parameters

Parameter	Range	Sampling point	
		Numbers	Values
C_{i-1}, C^i, C_i	0.10 - 2.00	10	0.1, 0.2, 0.3, 0.5, 0.7, 0.9, 1.2, 1.5, 1.8, 2.0
$R^{i-1}, R_{i-1}, R^i, R_i, R^{i+1}$	0.25 - 4.00	7	0.25, 0.33, 0.5, 1.0, 2.0, 3.0, 4.0
S_{i-1}/S_i	0.25 - 4.00	7	0.25, 0.33, 0.5, 1.0, 2.0, 3.0, 4.0
w_{i-1}/w_i	0.25 - 4.00	7	0.25, 0.33, 0.5, 1.0, 2.0, 3.0, 4.0

3. Selection of probable structural parameters

In order to cover a wide range of practical cases, it is required to define important parameters which could be varied to cover all practical situations and can be used as input parameters for generation of data sets.

As stated earlier, cracking in RC beams occurs near the internal supports (where hogging moments occur) and at in-span (where sagging moments occur) when elastic moments are higher than cracking moments. Owing to cracking, the moment of inertia of sections reduce from that of uncracked section, I^m to that of the cracked section, I^r , thereby reducing the stiffness of the spans. The elastic bending moment, M^{el} gets therefore redistributed and lead to inelastic bending moment, M^{in} .

It has been shown in earlier studies for continuous composite beams (Chaudhary *et al.* 2007, Pendharkar *et al.* 2007), that in order to establish redistribution of moment at any support with sufficient accuracy, cracking at the support and adjacent supports only needs to be considered. It is therefore assumed that in order to establish redistribution of moment at a support i in a RC continuous beam with sufficient accuracy, cracking at the support and adjacent supports and at the mid of adjacent spans only needs to be considered (Fig. 3). In the figure, superscript, i refers to the quantities at support i whereas, subscripts, $i-1$ or i refer to the quantities in spans $i-1$ or i . Fig. 3(a) shows an intermediate portion of a continuous beam with internal support i , and adjacent spans $i-1$ and i of lengths L_{i-1} and L_i subjected to loadings w_{i-1} and w_i respectively.

Considering the above discussion, the parameters affecting the redistribution of moments at a support i may be listed as

1. Inertia ratio at the support, C^i , where $C=I^r/I^g$ (I^r = transformed moment of inertia of RC section about neutral axis neglecting concrete in tension or cracked moment of inertia of RC section about neutral axis, and I^g = gross moment of inertia of RC section about neutral axis).
2. Inertia ratios at the mid of the spans, C_{i-1} and C_i .
3. Cracking moment ratios at the supports, R^{i-1} , R^i and R^{i+1} where $R=M^{cr}/M^{el}$.
4. Cracking moment ratios at the mid of the spans, R_{i-1} and R_i .
5. Stiffness ratio of adjacent spans, S_{i-1}/S_i ($S_i=E_c I^g/L_i$, where E_c = modulus of elasticity of concrete, and L_i = length of i^{th} span).
6. Load ratio of adjacent spans, w_{i-1}/w_i .

The moment at any cross-section along the length of a span can be obtained from the support moments and loading. Inelastic moment, $M^{in,j}$, at support i , may be obtained from elastic moment, $M^{el,j}$ and the inelastic moment ratio, $M^{el,j}/M^{in,j}$ at support i . The ratio $M^{el,i}/M^{in,i}$ would be the output

parameter, O for the neural networks. These ten input and one output parameters are schematically shown in Fig. 3(b). The practical ranges for the probable structural parameters are given in Table 1.

4. Data sets generation for neural networks

Since the training of the neural network is an essential step in its performance, a sufficiently large data set should be generated for training, validating, and testing. The performance in terms of generalization and prediction qualities of a neural network depends significantly on the training, validating, and testing data and the domain this data covers (Maru and Nagpal 2004).

It may be noted that the minimum number of spans in a continuous RC beam in which moment redistribution occurs is two. It may, further, be assumed that a beam with more than two spans would represent all the beams with three and larger number of spans. Presently, a representative beam having five spans is assumed to represent all beams having three and more spans. However, for continuous beams having more than two spans, non linear effects of cracking at penultimate and internal supports are different. It may further be assumed that the non linear effects of cracking at all internal supports are similar in beams having more than two spans. Accordingly, two separate data sets are generated for penultimate and internal supports of continuous beams having more than two spans. The penultimate supports of three span beams are assumed to be represented by penultimate supports of representative five span beam. One data set is separately generated for two span continuous beams. Hence, two sets of beams with number of spans equal to two and five may be considered to represent continuous composite beams with any number of spans.

First, consider the internal support ($i = 2$) of a two span continuous beam. Since moments at supports $i - 1$ and $i + 1$ are equal to zero, only eight input parameters (C_{i-1} , C^i , C_{i+1} , R_{i-1} , R^i , R_{i+1} , S_{i-1}/S_i , w_{i-1}/w_i) need be considered. Next, consider continuous beams having three and more spans. For internal supports, as discussed in section 3, ten input parameters are considered. For penultimate supports also, ten parameters are considered. In order to simulate values of moments at external supports equal to zero, constant high values ($= 20$) for R^{i-1} and R^{i+1} are specified.

The sampling points of each input parameter considered, for data generation, are shown in Table 1. A combination of sampling points of the input parameters and the corresponding resulting value of the output parameter comprises a data set.

For data generation, an analytical-numerical procedure (Patel *et al.* 2014) has been used. The training data sets have been generated for the combinations of the sampling points of input parameters shown in Table 1. The parameters C_{i-1} , C^i , C_{i+1} , S_{i-1}/S_i , w_{i-1}/w_i can be varied independently and assume values indicated in Table 1. However the parameters R^{i-1} , R_{i-1} , R^i , R_i , R^{i+1} are interdependent and it is difficult to vary these independently, therefore one parameter is varied independently and the other parameters are allowed to assume values in the practical range 0.25 - 4.00. The training sets in which the values of the other parameters fall outside the practical range 0.25 - 4.00 are not considered.

Three neural networks, one for two span beams and two for multi span (having three and larger number of spans) beams are trained. The neural network for two span beams is for the internal supports and is designated as NET-TI. The neural networks for internal and penultimate supports of multi span beams are designated NET-MI and NET-MP respectively. For data generation of NET-MI and NET-MP, five span continuous beams are considered.

If the parameters R^{i-1} , R_{i-1} , R^i , R_i , R^{i+1} could be varied independently, the upper limit to the number of possible data sets that can be generated for training, validating and testing of the

Table 2 Normalization factors for input and output parameters

Network	Parameters										
	Input									Output	
	C_{i-1}	C^i	C_i	R^{i-1}	R_{r-1}	R^i	R_r	R^{i+1}	S_{i-1}/S_i	w_{i-1}/w_i	$M^{el,i}/M^{in,i}$
NET-TI	2.0	2.0	2.0	-	4.0	4.0	4.0	-	4.0	4.0	2.25
NET-MI	2.0	2.0	2.0	4.0	4.0	4.0	4.0	4.0	4.0	4.0	2.25
NET-MP	2.0	2.0	2.0	4.0	4.0	4.0	4.0	4.0	4.0	4.0	2.25

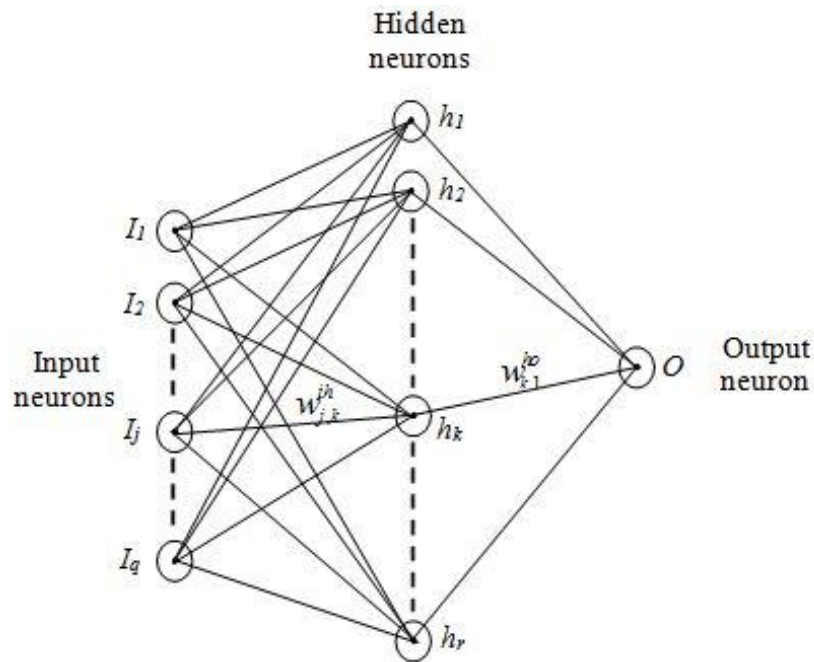


Fig. 4 Configuration of a typical neural network

networks NET-TI, NET-MI, and NET-MP would be 16,807,000 ($= 10 \times 10 \times 10 \times 7 \times 7 \times 7 \times 7 \times 7$), 823,543,000 ($= 10 \times 10 \times 10 \times 7 \times 7$) and 117,649,000 ($= 10 \times 10 \times 10 \times 7 \times 7 \times 7 \times 7 \times 7 \times 7$), respectively. As stated above if one of the parameters $R^{i-1}, R_{r-1}, R^i, R_r, R^{i+1}$ at a time is varied independently and the other parameters are constrained to assume values in the practical range 0.25 - 4.00, the number of data sets gets reduced to 89,349, 199,682 and 185,536 for networks NET-TI, NET-MI, and NET-MP respectively. In order to bring all the input and output parameters in the range 0.0 to 1.0, normalization factors are applied to the parameters. The normalization factors for input and output parameters are shown in Table 2.

5. Training, architecture and performance of neural networks

The neural networks chosen in the present study are multilayered feed-forward networks with neurons in all the layers fully connected in feed forward manner (Fig. 4). The training is carried

Table 3 Final architectures and statistical parameters of neural networks

Sets	Parameters	Network (Architecture)		
		NET-TI (8-10-1)	NET-MI (10-16-1)	NET-MP (10-16-1)
Training	MSE	0.00020	0.00010	0.00015
	R	0.99171	0.99573	0.99426
	RMSE	0.01414	0.01000	0.01225
	MAPE	2.74659	1.70130	2.20178
	AAD	2.49425	1.61497	2.04647
	COV	3.36310	2.18033	2.77475
Validating	MSE	0.00020	0.00010	0.00015
	R	0.99151	0.99567	0.99444
	RMSE	0.01424	0.01002	0.01224
	MAPE	2.76137	1.70930	2.20132
	AAD	2.50259	1.62443	2.04760
	COV	3.39545	2.18879	2.76660
Testing	MSE	0.00020	0.00010	0.00015
	R	0.99152	0.99578	0.99422
	RMSE	0.01442	0.01000	0.01239
	MAPE	2.79743	1.69556	2.21097
	AAD	2.53728	1.61376	2.06196
	COV	3.43025	2.18130	2.80723

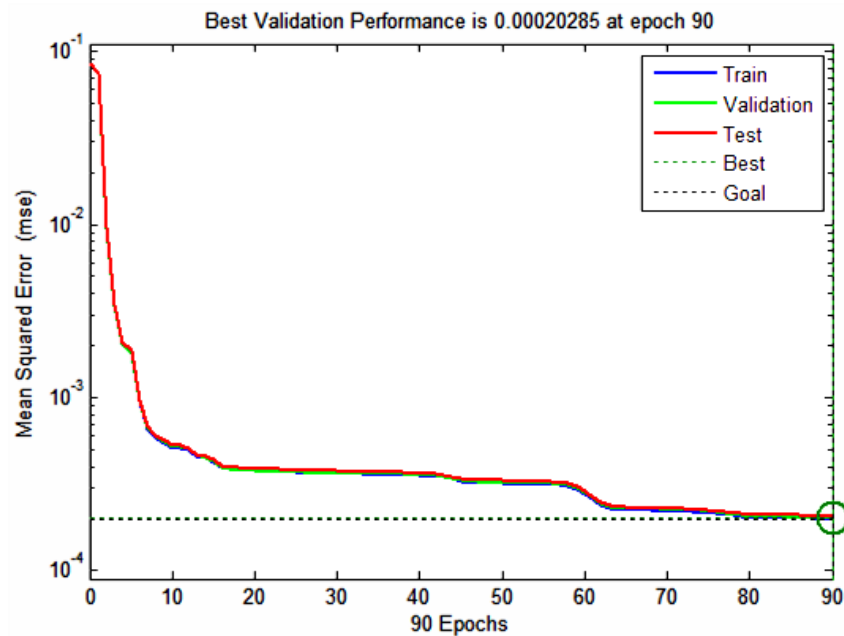


Fig. 5 Variation of the MSE with the epochs (iterations) for network NET-TI

out using the MATLAB Neural Network toolbox (2009). Sigmoid function is used as an activation function and the back propagation learning algorithm is used for training. One hidden layer is

chosen and the number of neurons in the layer is decided in the learning process by trial and error.

70% data sets are used for training and the remaining data sets are divided equally for validating and testing. For the training, several trials are carried out with different numbers of neurons in the hidden layer starting with a small number of neurons in the hidden layer and progressively increasing it and checking the mean square errors (MSE) of the training, the validation and the testing. The number of neurons in the hidden layer is decided on the basis of the least mean square errors (MSE) for the training, validation as well testing. Care is taken that the mean square error for test results does not increase with the number of neurons in hidden layer or epochs (overtraining). The final architectures (number of input parameters - number of neurons in the hidden layer - number of output parameters) of all networks along with the statistical parameters i.e. mean square error (MSE), coefficient of correlation (R), root mean square error (RMSE), mean absolute percentage error (MAPE), average absolute deviation (AAD) and percentage coefficient of variation (COV) of training, validating and testing data sets are given in Table 3. All the parameters indicate a good performance. Typically, for network NET-TI, variation of the MSE with the epochs (iterations) and regressions is shown in Figs. 5 and 6, respectively.

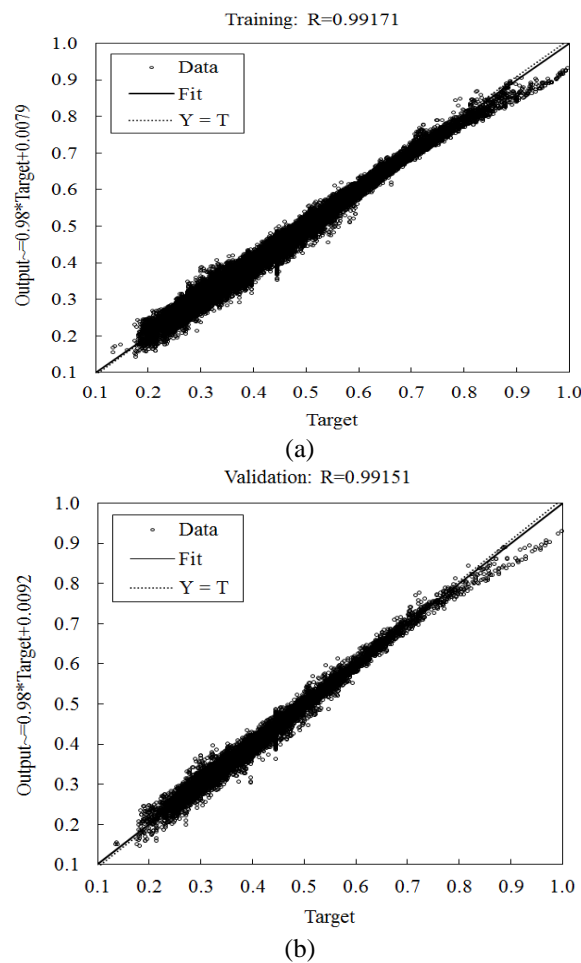
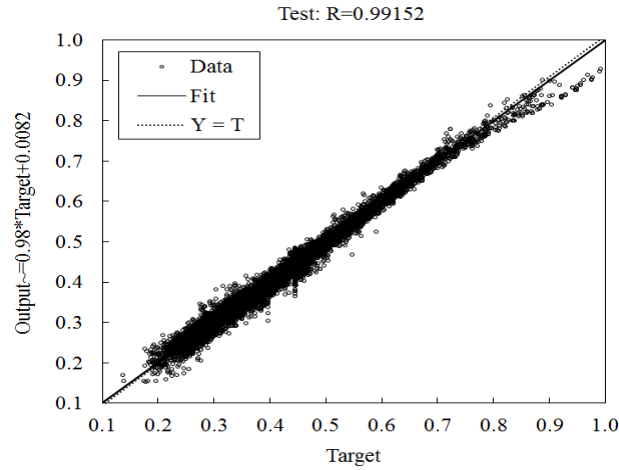
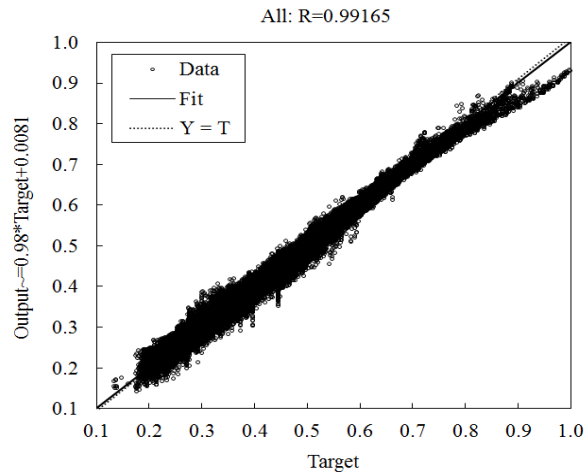


Fig. 6 Regressions of (a) training; (b) validation; (c) testing; and (d) all data sets for network NET-TI



(c)



(d)

Fig. 6 Continued

6. Closed form expressions

For the ease of practicing engineers and users, it is desirable to propose simplified closed form expressions, obtained from the trained neural networks, for the rapid prediction of inelastic bending moments. The closed form expressions require the values of inputs, weights of the links between the neurons in different layers, and biases of output neurons. Since the sigmoid functions have been used as the activation functions in the hidden and output layer neurons, the output O , ($=M^{el,i}/M^{in,i}$) is given as below (Tadesse *et al.* 2012, Gupta *et al.* 2013, 2015)

$$O = \frac{1}{1 + e^{-\left(bias_0 + \sum_{k=1}^r \frac{w_{k,1}^{ho}}{1 + e^{-H_k}} \right)}} \quad (1)$$

$$H_k = \sum_{j=1}^q w_{j,k}^{jh} \times I_j + bias_k \quad (2)$$

where, q is the number of input parameters; r is the number of hidden neurons; $bias_k$ is the bias of k^{th} hidden neuron (h_k); $bias_o$ is the bias of output neuron; $w_{j,k}^{jh}$ is the weight of the link between I_j and h_k ; $w_{k,1}^{ho}$ is the weight of the link between h_k and O . It has been established by researchers in previous studies that the weights and biases of trained networks define the relative importance of the input variables (Garson 1991, Olden and Jackson 2002, Olden *et al.* 2004).

The inelastic bending moment at support i is then given from Eq. (1) as

$$M^{in,i} = M^{el,i} / O \quad (3)$$

The value of O may be obtained from closed form expressions for internal supports of two span and multi span continuous beams and for penultimate supports of multi span continuous beams as given in Appendix A.

7. Verification of the proposed closed form expressions

The proposed closed form expressions are verified for five example beams with a wide variation of input parameters. The example beams (EB1-EB5) are shown schematically in Fig. 7. The cross-sectional properties (B_f = width of flange, D_f = depth of flange, B_w = width of web, D_w = depth of web, d_t = effective cover at top fibre, d_b = effective cover at top fibre) and E_c are given in Table 4. Additionally, the modulus of elasticity of steel reinforcements, $E_s = 205,000 \text{ N/mm}^2$, and tensile strength of concrete, $f_t = 0.623\sqrt{f_c}$ (ACI 318 2005) are taken. As shown in Table 4, three segments: left, middle, and right of lengths $0.25L_i$, $0.50L_i$ and $0.25L_i$ respectively, are assumed for reinforcement in each span. The reinforcement detailing data (area of top reinforcements, A_{st} and area of bottom reinforcements, A_{sb}) in each segment are also given in Table 4. Example beams have been chosen in such a way that none of the combinations of input parameters has been used in the training, validating and testing.

The inputs in the closed form expressions for the example beams are shown in Table 5. Inelastic moments, M^{in} obtained from finite element method (FEM), analytical-numerical procedure and proposed closed form expressions are reported in Table 6. For comparison, elastic moments, M^{el} are also reported.

For FEM analysis, modeling has been done in the ABAQUS (2011) software (Patel *et al.* 2014, 2015; Ramnavas *et al.* 2015). The beam is modelled using B21 elements (2-node linear Timoshenko beam element in plane). Under service load, the stress-strain relationship of concrete is assumed to be linear in compression. Concrete is considered as an elastic material in tension before cracking and softening behavior is assumed linearly after cracking (Patel *et al.* 2016). Tension stiffening is defined in the model using post-failure stress-strain data. In order to define the smeared crack model, the absolute value of the ratio of uniaxial tensile stress at failure to the uniaxial compressive stress at failure is obtained using concrete properties. The plastic strain is taken in accordance with tensile strength of concrete. Further, at service load, the stress in reinforcement is assumed to be in the linear range.

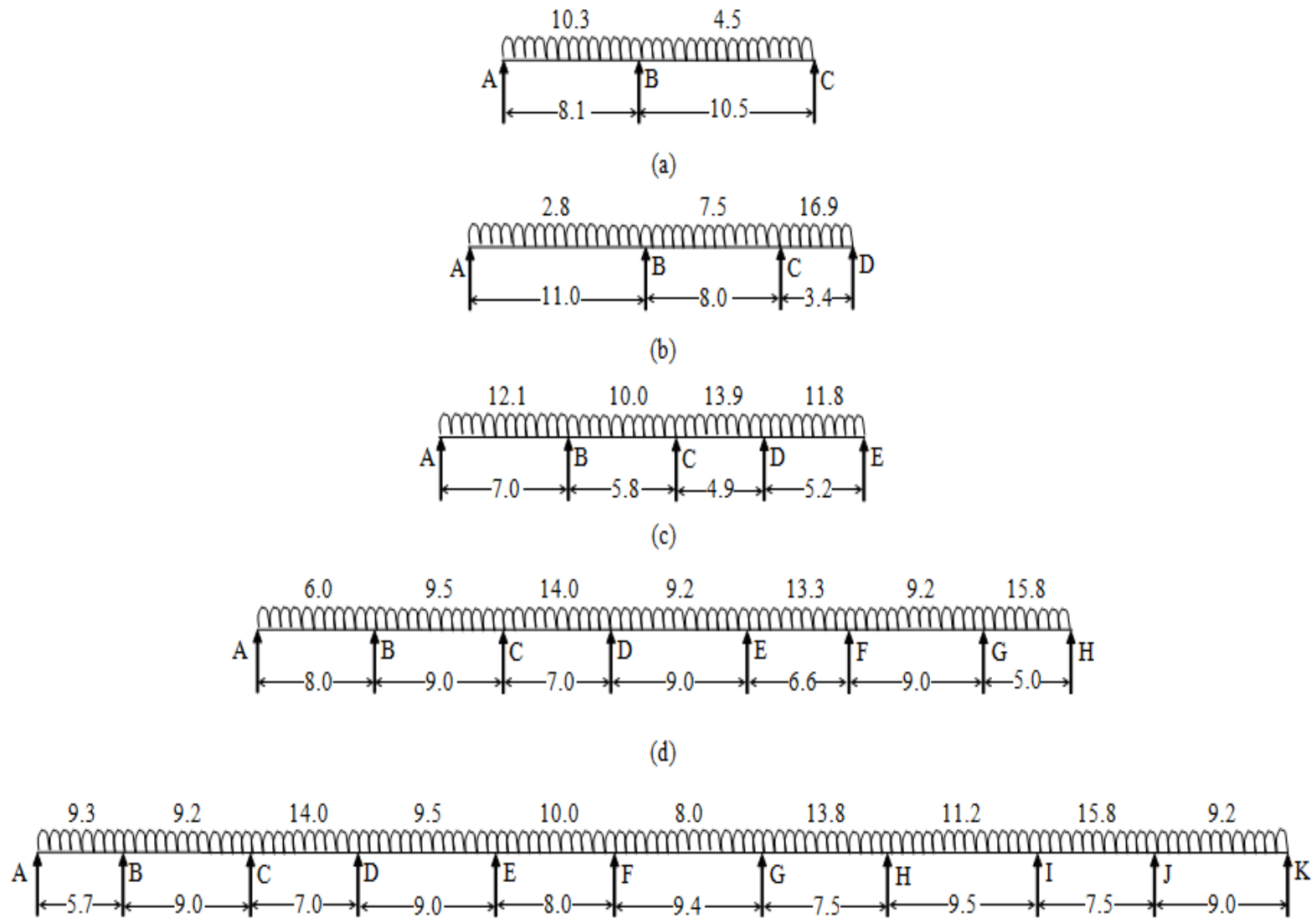


Fig. 7 Example beams: (a) EB1; (b) EB2; (c) EB3; (d) EB4; and (e) EB5 (span lengths in m and loads in kN/m)

Table 4 Properties of the example beams

Beams	B_f (mm)	D_f (mm)	B_w (mm)	D_w (mm)	$d_t=d_b$ (mm)	E_c (N/mm ²)	Segment (length)	Left (0.25 L_i)		Middle (0.50 L_i)		Right (0.25 L_i)	
							Span	A_{st} (mm ²)	A_{sb} (mm ²)	A_{st} (mm ²)	A_{sb} (mm ²)	A_{st} (mm ²)	A_{sb} (mm ²)
EB1	400	100	300	300	25	30,370	AB	157	402	157	402	509	226
							BC	509	226	157	402	157	402
EB2	-	-	230	450	25	27,335	AB	157	509	157	509	760	226
							BC	760	226	157	509	760	226
							CD	760	226	157	509	157	509
EB3	350	90	250	350	30	25,055	AB	157	226	157	226	226	157
							BC	226	157	157	226	226	157
							CD	226	157	157	226	226	157
							DE	226	157	157	226	157	226
EB4	-	-	300	300	27	31,900	AB	402	402	402	402	1,964	402
							BC	1,964	402	402	402	1,964	402
							CD	1,964	402	402	402	1,964	402
							DE	1,964	402	402	402	1,964	402
							EF	1,964	402	402	402	1,964	402
							FG	1,964	402	402	402	1,964	402
							GH	1,964	402	402	402	402	402
EB5	300	110	230	200	20	27,335	AB	226	760	226	760	1,964	760
							BC	1,964	760	226	760	1,964	760
							CD	1,964	760	226	760	1,964	760
							DE	1,964	760	226	760	1,964	760
							EF	1,964	760	226	760	1,964	760
				270			FG	1,964	760	226	760	1,964	760
							GH	1,964	760	226	760	1,964	760
							HI	1,964	760	226	760	1,964	760
							IJ	1,964	760	226	760	1,964	760
							JK	1,964	760	226	760	226	760

Table 5 Input parameters for the example beams

Beam	Used Neural Network	Support (i)	Input parameters									
			C_{i-1}	C^i	C_i	R^{i-1}	R_{i-1}	R^i	R_i	R^{i+1}	S_{i-1}/S_i	w_{i-1}/w_i
EB1	NET-TI	2	0.1645	0.1950	0.1645	-	0.7549	0.5786	1.4041	-	1.30	2.29
EB2	NET-MP	2	0.2780	0.3870	0.2780	20.000	1.4832	0.7736	1.4549	0.9564	0.73	0.37
	NET-MP	3	0.2780	0.3870	0.2780	0.7736	1.4549	0.9564	4.3505	20.000	0.43	0.44
EB3	NET-MP	2	0.1240	0.1199	0.1240	20.000	0.6543	0.6173	5.9921	1.8433	0.83	1.21
	NET-MI	3	0.1240	0.1199	0.1240	0.6173	5.9921	1.8433	2.1260	0.9433	0.84	0.72
	NET-MP	4	0.1240	0.1199	0.1240	1.8433	2.1260	0.9433	1.3968	20.000	1.06	1.18
EB4	NET-MP	2	0.2090	0.7160	0.2090	20.000	1.0652	0.4561	0.5683	0.4140	1.13	0.63
	NET-MI	3	0.2090	0.7160	0.2090	0.4561	0.5683	0.4140	0.8575	0.4255	0.78	0.68
	NET-MI	4	0.2090	0.7160	0.2090	0.4140	0.8575	0.4255	0.5898	0.4692	1.29	1.52
	NET-MI	5	0.2090	0.7160	0.2090	0.4255	0.5898	0.4692	1.2133	0.4660	0.73	0.69
	NET-MI	6	0.2090	0.7160	0.2090	0.4692	1.2133	0.4660	0.5838	0.4330	1.36	1.45
	NET-MP	7	0.2090	0.7160	0.2090	0.4660	0.5838	0.4330	1.0624	20.000	0.56	0.58
EB5	NET-MP	2	0.4740	0.9330	0.4740	20.000	1.5423	0.4728	0.4876	0.4063	1.58	1.01
	NET-MI	3	0.4740	0.9330	0.4740	0.4728	0.4876	0.4063	0.7231	0.4065	0.78	0.66
	NET-MI	4	0.4740	0.9330	0.4740	0.4063	0.7231	0.4065	0.4899	0.4213	1.29	1.47
	NET-MI	5	0.4740	0.9330	0.4740	0.4065	0.4899	0.4213	0.7644	0.4577	0.89	0.95
	NET-MI	6	0.4740	0.9330	0.4160	0.4213	0.7644	0.4577	0.8219	0.5952	1.18	1.25
	NET-MI	7	0.4160	0.8340	0.4160	0.4577	0.8219	0.5952	0.9091	0.4550	0.80	0.58
	NET-MI	8	0.4160	0.8340	0.4160	0.5952	0.9091	0.4550	0.5380	0.4468	1.27	1.23
	NET-MI	9	0.4160	0.8340	0.4160	0.4550	0.5380	0.4468	0.8608	0.4264	0.79	0.71
	NET-MP	10	0.4160	0.8340	0.4160	0.4468	0.8608	0.4264	0.4971	20.000	1.20	1.72

Table 6 Comparison of inelastic moments in the example beams

Beam	Support (i)	$M^{el,i}$ (kNm)	$M^{in,i}$ (kNm)		Error (%)
			FEM	NN	
EB1	2	71.80	69.59	69.60	-0.01
EB2	2	42.53	39.88	39.71	0.43
	3	34.40	32.90	30.97	5.87
EB3	2	55.27	54.08	51.35	5.05
	3	18.51	16.78	16.79	-0.06
	4	36.17	34.90	35.55	-1.86
EB4	2	56.53	64.84	63.88	1.48
	3	62.29	67.21	67.74	-0.79
	4	60.60	65.52	66.27	-1.14
	5	54.96	61.24	62.76	-2.48
	6	55.33	60.12	62.62	-4.16
EB5	7	59.55	67.08	67.55	-0.70
	2	52.81	57.04	57.70	-1.16
	3	61.45	64.00	63.63	0.58
	4	61.43	64.33	67.40	-4.77
	5	59.27	62.19	61.62	0.92
	6	54.56	57.10	54.25	4.99
	7	59.48	61.57	63.38	-2.94
	8	77.80	86.41	82.29	4.77
	9	79.23	84.70	82.99	2.02
	10	83.02	97.29	94.61	2.75

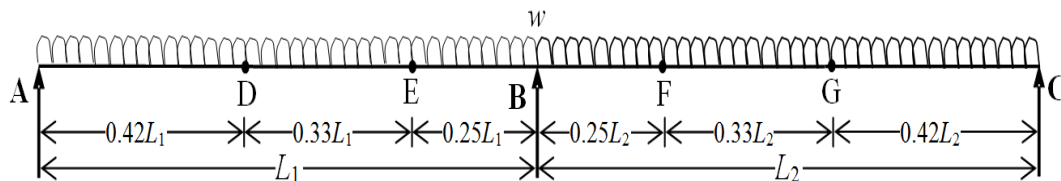


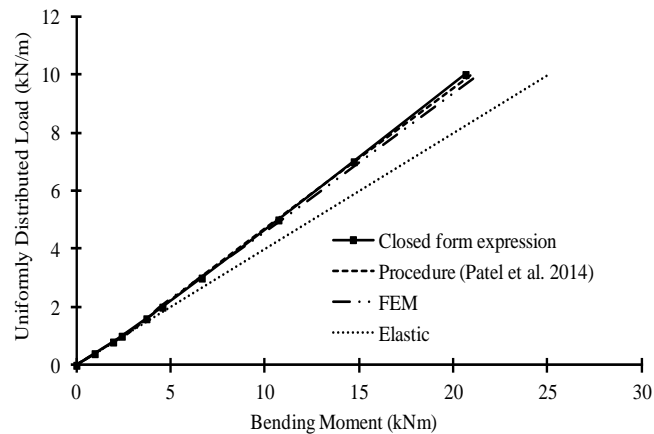
Fig. 8 Two span continuous beam

The maximum absolute percentage errors for beams EB1-EB5 are 0.01%, 5.87%, 5.05%, 4.16% and 4.99% respectively as shown in Table 6. The root mean square percentage error for all the beams is 2.97%. This shows the efficacy of the developed methodology for continuous beams with any number of spans.

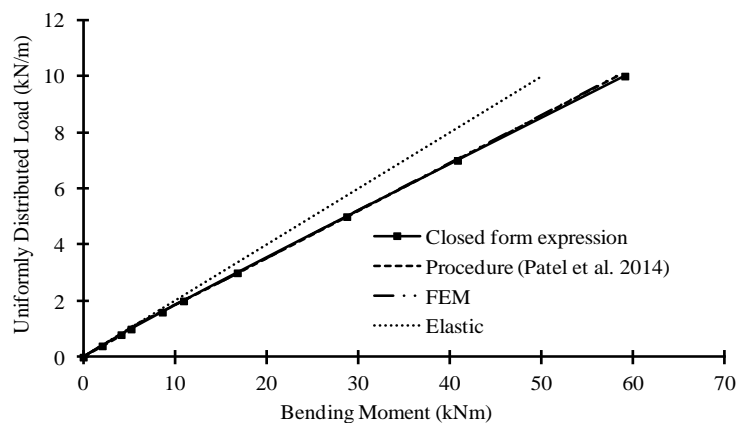
Further, in order to validate the proposed closed form expression for inelastic bending moments with increasing uniformly distributed load, w , a two span continuous beam EB6 is considered (Fig. 8). The properties are: $L_1 = L_2 = 6.34$ m, $B_w = 304.8$ mm, $D_w = 127$ mm, $d_t = d_b = 24$ mm, $E_c = 23,270$ N/mm², $E_s = 206,843$ N/mm², $f_t = 3.27$ N/mm², $A_{st} = A_{sb} = 1,000$ mm² in segment EF and $A_{st} = A_{sb} = 516$ mm² in segments AE, FC. Bending moment at the centre of span AB and at support B obtained from the proposed closed form expression, the analytical-numerical procedure (Patel *et al.* 2014) and FEM are shown in Fig. 9. Inelastic bending moments at the centre of span AB are obtained using the moments at support B, loading and span length. Also shown, for comparison, are the elastic bending moments obtained neglecting cracking. Close agreement is observed

between the results obtained using the proposed closed form expression, the analytical-numerical procedure (Patel *et al.* 2014) and FEM.

The procedures available in literature or any other commercial software based on finite element analysis that incorporate concrete cracking would require reinforcement detailing data. In finite element analysis, usually 16-32 elements in a span are required for convergence of results within 1% (Patel *et al.* 2014). It would be tedious to provide such reinforcement detailing data for every element in a large structure since reinforcement lengths and cross-section areas may vary from element to element. On the other hand, the present methodology requires only cross sectional properties, elastic moments and reinforcement data at three locations. When the closed form expressions are used, the computational time is drastically reduced and it is a fraction of that required for finite element analysis and other procedures available in literature.



(a)



(b)

Fig. 9 Comparison of bending moments at: (a) centre of span AB (sagging), and (b) support B (hogging) in beam EB6

8. Conclusions

Closed form expressions, obtained from the trained neural networks, have been proposed for rapid prediction of the inelastic bending moments in continuous RC beams subjected to service load. The expressions take into account the concrete cracking and tension stiffening effect. Three separate neural networks (NET-TI, NET-MI, and NET-MP) are developed for prediction of inelastic moments (due to concrete cracking and tension stiffening) from the elastic moments (neglecting concrete cracking) for continuous RC beams having any number of spans. Data sets for training, validating, and testing for neural networks are generated using the computationally efficient analytical-numerical procedure recently developed by authors. The proposed expressions have been verified for a number of example beams. The maximum absolute error for any span in the example beams is 5.87% and root mean square error of all spans of all beams is 2.97%. The proposed expressions require minimal input data and computation effort and yield results that are close to FEM results. The expressions can be used in preliminary every day design since the required computational effort is a fraction of that required for the available methods.

The methodology can be extended for large RC building frames where a very significant saving in computational effort would result. The methodology can also be extended to account for shear deformation in RC beams with low span-effective depth ratios (Wang *et al.* 2015).

References

- ABAQUS (2011), ABAQUS standard user's manuals, Version 6.11, Hibbitt, Karlsson and Sorensen, Inc., Pawtucket, RI, USA.
- ACI 318 (2005), Building code requirements for structural concrete and commentary, American Concrete Institute (ACI) Committee 318, USA.
- Bathe, K.J. (2002), Finite element procedures, (6th Edition), Prentice-Hall Pvt. Ltd., New Delhi, India.
- Caglar, N., Pala, M., Elmas, M. and Eryılmaz, D.M. (2009), "A new approach to determine the base shear of steel frame structures", *J. Constr. Steel Res.*, **65**(1), 188-195.
- Casanova, A., Jason, L. and Davenne, L. (2012), "Bond slip model for the simulation of reinforced concrete structures", *Eng. Struct.*, **39**, 66-78.
- Chan, C.M., Mickleborough, N.C. and Ning, F. (2000), "Analysis of cracking effects on tall reinforced concrete buildings", *J. Struct. Eng.*, **126**(9), 995-1003.
- Chan, C.M., Ning, F. and Mickleborough, N.C. (2000), "Lateral stiffness characteristics of tall reinforced concrete buildings under service loads", *Struct. Des. Tall Build.*, **9**(5), 365-383.
- Chaudhary, S., Pendharkar, U. and Nagpal, A.K. (2007), "Bending moment prediction for continuous composite beams by neural networks", *Adv. Struct. Eng.*, **10**(4), 439-454.
- Chaudhary, S., Pendharkar, U., Patel, K.A. and Nagpal, A.K. (2014), "Neural networks for deflections in continuous composite beams considering concrete cracking", *Iran. J. Sci. Tech. Transact. Civil Eng.*, **38**(C1+), 205.
- Dai, J.G., Ueda, T., Sato, Y. and Nagai, K. (2012), "Modeling of tension stiffening behavior in FRP-strengthened RC members based on rigid body spring networks", *Comput-Aid. Civil Infrastruct. Eng.*, **27**(6), 406-418.
- Dias, J.L.R. and Silvestre, N. (2011), "A neural network based closed-form solution for the distortional buckling of elliptical tubes", *Eng. Struct.*, **33**(6), 2015-2024.
- Dundar, C. and Kara, I.F. (2007), "Three dimensional analysis of reinforced concrete frames with cracked beam and column elements", *Eng. Struct.*, **29**(9), 2262-2273.
- Garson, G.D. (1991), "Interpreting neural-network connection weights", *AI Expert*, **6**(7), 47-51.

- Gupta, R.K., Kumar, S., Patel, K.A., Chaudhary, S. and Nagpal, A.K. (2015), "Rapid prediction of deflections in multi-span continuous composite bridges using neural networks", *Int. J. Steel Struct.*, **15**(4), 893-909.
- Gupta, R.K., Patel, K.A., Chaudhary, S. and Nagpal, A.K. (2013), "Closed form solution for deflection of flexible composite bridges", *Proc. Eng.*, **51**, 75-83.
- Joshi, S.G., Londhe, S.N. and Kwatra, N. (2014), "Application of artificial neural networks for dynamic analysis of building frames", *Comput. Concrete*, **13**(6), 765-780.
- Kara, I.F. and Dundar, C. (2009), "Effect of loading types and reinforcement ratio on an effective moment of inertia and deflection of a reinforced concrete beam", *Adv. Eng. Softw.*, **40**(9), 836-846.
- Kara, I.F. and Dundar, C. (2010), "Three-dimensional analysis of tall reinforced concrete buildings with nonlinear cracking effects", *Mech. Based Des. Struct. Mach.*, **38**(3), 388-402.
- Khan, M.I. (2012), "Predicting properties of high performance concrete containing composite cementitious materials using artificial neural networks", *Automat. Constr.*, **22**, 516-524.
- Kim, D.K., Kim, D.H., Cui, J., Seo, H.Y. and Lee, Y.H. (2009), "Iterative neural network strategy for static model identification of an FRP deck", *Steel Comp. Struct.*, **9**(5), 445-455.
- Maru, S. and Nagpal, A.K. (2004), "Neural network for creep and shrinkage deflections in reinforced concrete frames", *J. Comput. Civil Eng.*, **18**(4), 350-359.
- MATLAB 7.8. (2009), Neural networks toolbox user's guide, The Mathworks Inc., USA.
- Mohammadhassani, M., Nezamabadi-Pour, H., Jumaat, M.Z., Jameel, M. and Arumugam, A.M.S. (2013a), "Application of artificial neural networks (ANNs) and linear regressions (LR) to predict the deflection of concrete deep beams", *Comput. Concrete*, **11**(3), 237-252.
- Mohammadhassani, M., Nezamabadi-Pour, H., Jumaat, M.Z., Jameel, M., Hakim, S.J.S. and Zargar, M. (2013b), "Application of the ANFIS model in deflection prediction of concrete deep beam", *Struct. Eng. Mech.*, **45**(3), 319-332.
- Mohr, S., Bairán, J.M. and Marí, A.R. (2010), "A frame element model for the analysis of reinforced concrete structures under shear and bending", *Eng. Struct.*, **32**(12), 3936-3954.
- Olden, J.D. and Jackson, D.A. (2002), "Illuminating the "black box": a randomization approach for understanding variable contributions in artificial neural networks", *Ecol. Model.*, **154**(1), 135-150.
- Olden, J.D., Joy, M.K. and Death, R.G. (2004). "An accurate comparison of methods for quantifying variable importance in artificial neural networks using simulated data", *Ecol. Model.*, **178**(3), 389-397.
- Pala, M. (2006), "A new formulation for distortional buckling stress in cold-formed steel members", *J. Constr. Steel Res.*, **62**(7), 716-722.
- Patel, K.A., Bhardwaj, A., Chaudhary, S. and Nagpal, A.K. (2015), "Explicit expression for effective moment of inertia of RC Beams", *Lat. Am. J. Solid Struct.*, **12**(3), 542-560.
- Patel, K.A., Chaudhary, S. and Nagpal, A.K. (2016), "A tension stiffening model for analysis of reinforced concrete flexural members subjected to service load", *Comput. Concrete*, **17**(1), 29-51.
- Patel, K.A., Chaudhary, S. and Nagpal, A.K. (2014), "Analytical-numerical procedure incorporating cracking in RC beams", *Eng. Comput.*, **31**(5), 986-1010.
- Pendharkar, U., Chaudhary, S. and Nagpal, A.K. (2007), "Neural network for bending moment in continuous composite beams considering cracking and time effects in concrete", *Eng. Struct.*, **29**(9), 2069-2079.
- Pendharkar, U., Chaudhary, S. and Nagpal, A.K. (2010), "Neural networks for inelastic mid-span deflections in continuous composite beams", *Struct. Eng. Mech.*, **36**(2), 165-179.
- Pendharkar, U., Chaudhary, S. and Nagpal, A.K. (2011), "Prediction of moments in composite frames considering cracking and time effects using neural network models", *Struct. Eng. Mech.*, **39**(2), 267-285.
- Pendharkar, U., Patel, K.A., Chaudhary, S. and Nagpal, A.K. (2015), "Rapid prediction of long-term deflections in composite frames", *Steel Compos. Struct.*, **18**(3), 547-563.
- Ramnavas, M.P., Patel, K.A., Chaudhary, S. and Nagpal, A.K. (2015), "Cracked span length beam element for service load analysis of steel concrete composite bridges", *Comput. Struct.*, **157**, 201-208.
- Saechai, S., Kongprawechnon, W. and Sahamitmongkol, R. (2012), "Test system for defect detection in construction materials with ultrasonic waves by support vector machine and neural network", *Proceedings*

- International SCIS-ISIS Conference*, 1034-1039.
- Saechai, S., Kusalanggoorawat, P., Kongprawechnon, W. and Sahamitmongkol, R. (2011), "New developed testing system of defect in cementitious material with neural network", *Proceedings of 8th International ECTI Conference*, 565-568.
- Shahin, M. and Elchanakani, M. (2008), "Neural networks for ultimate pure bending of steel circular tubes", *J. Constr. Steel Res.*, **64**(6), 624-633.
- Stramandinoli, R.S.B. and Rovere, H.L.L. (2008), "An efficient tension-stiffening model for nonlinear analysis of reinforced concrete members", *Eng. Struct.*, **30**(7), 2069-2080.
- Stramandinoli, R.S.B. and Rovere, H.L.L. (2012), "FE model for nonlinear analysis of reinforced concrete beams considering shear deformation", *Eng. Struct.*, **35**, 244-253.
- Tadesse, Z., Patel, K.A., Chaudhary, S. and Nagpal, A.K. (2012), "Neural networks for prediction of deflection in composite bridges", *J. Constr. Steel Res.*, **68**(1), 138-149.
- Tanrikulu, A.K., Dundar, C. and Cagatay, I.H. (2000), "A computer program for the analysis of reinforced concrete frames with cracked beam elements", *Struct. Eng. Mech.*, **10**(5), 463-478.
- Tohidi, S. and Sharifi, Y. (2015), "Neural networks for inelastic distortional buckling capacity assessment of steel I-beams", *Thin Wall Struct.*, **94**, 359-371.
- Varshney, L.K., Patel, K.A., Chaudhary, S. and Nagpal, A.K. (2013), "Control of time-dependent effects in steel-concrete composite frames", *Int. J. Steel Struct.*, **13**(4), 589-606.
- Wang, T. and Hsu, T.T.C. (2001), "Nonlinear finite element analysis of concrete structures using new constitutive models", *Comput. Struct.*, **79**(32), 2781-2791.
- Wang, T., Dai, J.G. and Zheng, J.J. (2015), "Multi-angle truss model for predicting the shear deformation of RC beams with low span-effective depth ratios", *Eng. Struct.*, **91**, 85-95.
- Yang, Z.J. and Chen, J. (2005), "Finite element modelling of multiple cohesive discrete crack propagation in reinforced concrete beams", *Eng. Fract. Mech.*, **72**(14), 2280-2297.

CC

Notation

- s : reinforcement spacing;
- A_{st}, A_{sb} : area of top and bottom reinforcement respectively;
- B, D : width, and total depth of section respectively;
- f_s : stress in steel reinforcement on tension face;
- d_t, d_b : effective concrete cover at top and bottom respectively;
- E : modulus of elasticity;
- f_t, f_c' : tensile strength and cylinder compressive strength respectively;
- L : length of the span;
- M : bending moment;
- C, R : inertia ratio and cracking moment respectively;
- S : stiffness;
- h_k : k^{th} hidden neuron;
- q : number of input parameters;
- r : number of hidden neurons;
- $w_{j,k}^{ih}$: weight of the link between I_j and h_c ;
- $w_{k,1}^{ho}$: weight of the link between h_c and O ;

w	uniformly distributed load;
x	: crack length;
O	: output parameter;
I_j	: j^{th} input parameter;
bias	: bias of hidden or output neuron;
I	: moment of inertia about neutral axis.
<i>Subscript</i>	
A, B	: ends A and B of a cracked span length beam element;
S	: in-span position of a cracked span length beam element;
c, s	: concrete and steel respectively;
j	: input neuron number;
k	: hidden neuron number or function number;
o	: output neuron number;
i	: i^{th} span;
f, w	: flange and web respectively.
<i>Superscript</i>	
in	: inelastic;
el	: elastic;
cr, un	: cracked and uncracked respectively;
g	: gross;
i	: i^{th} support;
ho	: connection between hidden and output layers;
ih	: connection between input and hidden layers.

Appendix A: Closed form expressions for value of O

(I) Internal support of two span continuous beams

$$O = \left[\frac{2.25}{1+e^{-\left(10.11 - \frac{50.08}{1+e^{-H_1}} + \frac{13.71}{1+e^{-H_2}} + \frac{18.31}{1+e^{-H_3}} + \frac{0.66}{1+e^{-H_4}} + \frac{3.10}{1+e^{-H_5}} + \frac{0.82}{1+e^{-H_6}} + \frac{1.65}{1+e^{-H_7}} + \frac{2.13}{1+e^{-H_8}} + \frac{4.07}{1+e^{-H_9}} + \frac{1.12}{1+e^{-H_{10}}}\right)}} \right] \quad (A1)$$

$$\begin{bmatrix} H_1 \\ H_2 \\ H_3 \\ H_4 \\ H_5 \\ H_6 \\ H_7 \\ H_8 \\ H_9 \\ H_{10} \end{bmatrix} = \begin{bmatrix} -0.38 & 10.32 & -0.64 & -0.55 & 8.96 & -0.38 & 0.58 & -0.17 \\ -0.53 & 11.42 & -0.85 & -0.84 & 8.26 & -0.55 & 0.99 & -0.29 \\ -1.35 & 2.64 & 6.76 & 0.50 & 12.71 & 0.90 & -4.02 & 1.20 \\ 3.77 & 1.10 & -3.66 & -1.24 & -0.67 & 2.18 & 1.64 & 0.20 \\ 1.54 & -2.00 & 0.17 & -1.12 & -3.85 & -0.01 & 3.94 & -1.48 \\ -2.04 & 3.55 & -2.05 & 0.79 & -14.69 & 0.32 & -3.19 & 1.29 \\ 0.66 & 0.60 & -10.14 & -6.73 & 1.40 & 1.34 & -1.94 & 1.06 \\ -2.77 & 2.45 & 0.30 & 2.10 & -1.46 & -0.25 & -7.16 & 2.57 \\ 7.25 & 4.00 & -1.17 & 1.00 & 20.55 & -0.48 & 1.12 & -0.02 \\ 12.25 & -0.66 & -0.81 & -1.52 & -1.29 & 7.78 & -1.76 & 1.27 \end{bmatrix} \begin{bmatrix} C_{i-1} \\ C^i \\ C_i \\ R_{i-1} \\ R^i \\ R_i \\ S_{i-1}/S_i \\ w_{i-1}/w_i \end{bmatrix} + \begin{bmatrix} 2.05 \\ 1.34 \\ 3.04 \\ 0.66 \\ -0.80 \\ 1.40 \\ -1.21 \\ 1.66 \\ -0.16 \\ 0.98 \end{bmatrix} \quad (A2)$$

(II) Internal supports of multi span continuous beams

$$O = \left[\frac{2.25}{1+e^{-\left(11.40 - \frac{7.82}{1+e^{-H_1}} + \frac{9.96}{1+e^{-H_2}} + \frac{1.98}{1+e^{-H_3}} + \frac{9.02}{1+e^{-H_4}} + \frac{3.00}{1+e^{-H_5}} + \frac{16.90}{1+e^{-H_6}} + \frac{25.27}{1+e^{-H_7}} + \frac{16.40}{1+e^{-H_8}} + \frac{0.91}{1+e^{-H_9}} + \frac{15.81}{1+e^{-H_{10}}} + \frac{19.00}{1+e^{-H_{11}}} + \frac{17.08}{1+e^{-H_{12}}} + \frac{2.73}{1+e^{-H_{13}}} + \frac{7.42}{1+e^{-H_{14}}}\right)}} \right] \quad (A3)$$

$$\begin{bmatrix} H_1 \\ H_2 \\ H_3 \\ H_4 \\ H_5 \\ H_6 \\ H_7 \\ H_8 \\ H_9 \\ H_{10} \\ H_{11} \\ H_{12} \\ H_{13} \\ H_{14} \end{bmatrix} = \begin{bmatrix} -0.23 & 1.30 & -0.66 & -0.61 & -1.87 & -3.41 & 7.76 & -0.35 & -1.75 & 0.36 \\ 0.09 & 0.23 & 0.02 & -0.70 & -1.28 & -1.43 & 8.83 & -1.93 & -0.87 & 0.11 \\ 2.99 & 0.73 & -1.87 & 4.10 & -2.94 & 0.18 & -0.72 & 5.67 & -2.03 & -0.42 \\ 0.91 & -1.32 & -0.42 & 1.21 & -0.52 & -2.93 & -0.03 & -0.38 & 1.07 & -0.17 \\ -1.40 & 0.69 & -1.81 & -5.40 & -0.36 & -2.33 & 0.69 & -4.38 & -2.14 & 0.69 \\ 0.32 & -1.56 & 0.41 & 0.59 & -0.35 & -3.11 & -0.48 & 1.01 & 0.20 & -0.11 \\ 0.62 & -17.93 & 0.55 & 1.63 & -0.30 & -17.84 & -0.10 & 1.18 & -0.25 & 0.10 \\ 1.30 & -0.14 & -1.11 & -0.05 & -0.36 & 1.29 & -0.10 & 1.74 & 1.54 & -0.26 \\ 0.18 & -0.04 & 8.40 & -7.17 & 21.74 & -2.42 & 0.38 & -2.66 & 3.83 & -0.43 \\ 0.05 & 1.18 & -0.84 & -0.37 & 0.25 & 3.06 & 0.60 & -1.72 & 0.43 & 0.02 \\ 0.02 & 0.51 & -0.24 & -0.65 & -1.40 & -1.98 & 7.97 & -1.28 & -1.20 & 0.21 \\ 0.93 & -0.12 & -1.37 & -1.09 & -0.08 & 1.27 & 0.09 & 0.59 & 1.23 & -0.15 \\ 1.34 & 1.56 & 0.41 & 5.47 & -0.73 & -0.37 & -1.08 & 5.72 & 1.65 & -0.64 \\ -10.47 & -0.20 & -0.15 & -1.84 & 2.36 & 1.44 & -0.66 & -8.68 & 1.30 & -0.82 \end{bmatrix} \begin{bmatrix} C_{i-1} \\ C^i \\ C_i \\ R^{i-1} \\ R_{i-1} \\ R^i \\ R_i \\ R^{i+1} \\ S_{i-1}/S_i \\ w_{i-1}/w_i \end{bmatrix} + \begin{bmatrix} 1.84 \\ -0.20 \\ -5.09 \\ -0.05 \\ 1.85 \\ 0.71 \\ -1.91 \\ -0.81 \\ -1.21 \\ -0.19 \\ 0.63 \\ -0.02 \\ -4.83 \\ -2.96 \end{bmatrix} \quad (A4)$$

(III) Penultimate supports of multi span continuous beams

$$O = \left[\frac{2.25}{1+e^{-\left(\frac{-13.37}{1+e^{-H_1}} + \frac{44.84}{1+e^{-H_2}} + \frac{29.44}{1+e^{-H_3}} + \frac{3.65}{1+e^{-H_4}} + \frac{43.73}{1+e^{-H_5}} + \frac{5.81}{1+e^{-H_6}} + \frac{8.24}{1+e^{-H_7}} + \frac{0.30}{1+e^{-H_8}} + \frac{0.63}{1+e^{-H_9}} + \frac{8.22}{1+e^{-H_{10}}} + \frac{26.74}{1+e^{-H_{11}}} + \frac{6.53}{1+e^{-H_{12}}} + \frac{18.18}{1+e^{-H_{13}}} + \frac{15.92}{1+e^{-H_{14}}} + \frac{24.22}{1+e^{-H_{14}}} \right)} \right] \quad (A5)$$

$$\begin{bmatrix} H_1 \\ H_2 \\ H_3 \\ H_4 \\ H_5 \\ H_6 \\ H_7 \\ H_8 \\ H_9 \\ H_{10} \\ H_{11} \\ H_{12} \\ H_{13} \\ H_{14} \end{bmatrix} = \begin{bmatrix} 3.84 & -0.15 & -0.43 & -0.53 & 0.67 & -0.63 & 2.92 & -0.40 & -0.01 & 0.25 \\ -0.35 & 1.86 & -0.02 & 0.23 & -0.30 & 5.17 & -0.28 & 0.22 & -0.05 & 0.05 \\ 0.25 & -1.97 & -6.06 & -2.50 & 0.52 & 4.71 & -9.95 & -2.22 & 2.44 & -0.45 \\ -0.34 & 19.87 & -0.63 & -0.08 & -0.13 & 17.29 & 0.05 & -0.07 & 0.64 & -0.28 \\ 1.15 & -3.08 & 0.52 & -1.63 & -2.30 & 1.85 & -1.71 & -1.56 & 3.68 & -1.57 \\ 1.14 & -0.26 & -2.96 & 5.86 & -5.25 & 2.51 & -3.60 & -1.82 & -3.43 & 0.87 \\ 2.89 & 10.46 & -1.45 & -2.28 & 1.80 & 19.02 & 0.33 & -2.17 & 0.08 & 0.00 \\ 1.59 & -3.88 & 1.46 & -0.23 & -0.50 & 16.57 & 0.80 & -0.13 & 3.74 & -1.62 \\ -3.09 & 0.17 & 0.79 & 1.78 & -2.53 & 0.68 & -3.89 & 4.69 & 0.78 & -0.72 \\ -1.92 & -0.16 & -1.66 & -2.01 & -0.15 & 0.71 & -0.21 & -1.98 & 0.32 & -0.22 \\ -1.18 & 3.23 & -0.47 & 1.53 & 1.98 & -2.18 & 1.33 & 1.46 & -3.70 & 1.58 \\ 5.62 & 1.22 & -0.57 & 1.12 & 7.44 & -3.41 & 0.67 & 1.19 & 1.24 & 0.20 \\ 5.93 & 0.77 & -0.72 & 1.48 & 5.54 & -3.00 & 1.55 & 1.53 & 1.49 & 0.08 \\ -0.47 & -0.04 & 3.46 & -1.36 & 3.79 & -1.06 & 0.43 & -1.55 & 1.44 & -0.34 \end{bmatrix} + \begin{bmatrix} C_{i-1} \\ C^i \\ C_i \\ R^{i-1} \\ R_{i-1} \\ R^i \\ R_i \\ R^{i+1} \\ S_{i-1}/S_i \\ w_{i-1}/w_i \end{bmatrix} = \begin{bmatrix} 5.26 \\ 1.87 \\ 10.90 \\ 2.59 \\ 9.26 \\ 7.39 \\ 6.96 \\ -1.02 \\ -10.93 \\ 7.26 \\ -8.48 \\ -5.50 \\ -7.24 \\ 10.18 \end{bmatrix} \quad (A6)$$